Electronic Supplementary Material (ESI) for ChemComm.

Supporting information

The secondary coordination sphere controlled reactivity of a ferric-superoxo heme: Unexpected conversion to a ferric hydroperoxo intermediate by a reaction with a high-spin ferrous heme

Perumandla Nagaraju,[a,c] Takehiro Ohta,[b,c,*] Jin-Gang Liu,[d] Takashi Ogura[b] and Yoshinori Naruta[a,c,*]

[a] *Institute of Science and Technology Research, Chubu University, Kasugai, Aichi 487-8501, Japan. Email: naruta@isc.chubu.ac.jp*

[b] *Picobiology Institute, Graduate School of Life Science, University of Hyogo, Hyogo 679-5148, Japan.*

Email: takehiro@sci.u-hyogo.ac.jp

[c] *Institute for Materials Chemistry and Engineering, Kyushu University, Fukuoka 812-8581, Japan.*

[d] *Department of Chemistry, East China University of Science and Technology, 20237 Shanghai, China.*

General

All reagents and solvents were obtained commercially and used without further purification unless otherwise noted. Tetrahydrofuran (THF) was pre-dried over KOH and distilled from Na/benzophenone under N_2 atmosphere. Acetonitrile (CH_3CN) for spectroscopic measurements was purified as follows: It was first distilled from P_2O_5 and redistilled from CaH_2. After being degassed three times by freeze-thaw method, it was stirred over KO_2 (Aldrich) for ca. 1 h and then passed through activated alumina (Wako) which was dried in prior at 120 ^oC under vacuum for 10 h. Subsequently, it was degassed three times by freeze-thaw technique again. The other degassed solvents were also treated by freeze-thaw method. Preparation and handling of air sensitive materials were carried out under N_2 in a glove-box (M. Braun 150B-G-II) equipped with a circulating purifier (O_2, H_2O < 1 ppm). Cobaltocene ($CoCp_2$) was freshly sublimed (>40°C) under vacuum before use.

Instruments and Methods

^1H NMR spectra were recorded on a JEOL LMX-GX 400 (400 MHz) spectrometer. Chemical shift was referenced to the residual solvent signal. Electrospray ionization mass (ESI-MS) spectra were obtained on a Perkin-Elmer Sciex API-300 mass spectrometer. Scanning was in 0.1-dalton steps and a 10-ms dwell time per step. The orifice voltage was controlled from -20 to +180 V, dependent on the intensity of TIC. High-resolution mass (HR-MS) spectra were recorded on a JEOL LMS-HX-110 spectrometer with 3-nitrobenzyl alcohol (NBA) as a matrix.

The UV-vis electronic spectra were recorded on a Hamamatsu PMA-11 CCD spectrophotometer with a Photal MC-2530 (D_2/W_2) as a light source. The temperature was controlled by a NESLAB ULT-95 low temperature circulator. To a degassed solution of model compound (~ 10^{-4} M) in a 0.2-cm UV cuvette, dry O_2 gas through molecular sieves was introduced into the solution with O_2 line. Its spectral change was monitored by an UV-vis spectrometer. After formation of the heme-superoxide (**2a**, **2b),** excess O_2 was removed from the UV cuvette by evacuating the headspace and backfilling with N_2 (5×). A solution of $CoCp_2$ and Fe^{II}- reduced form in THF (1.0 equiv.) was then added to the resultant solution of compound (**2a**, **2b)** at –70 ^oC and its UV-vis spectral change was recorded.

ESR spectra were obtained at 77 K in a 5.0-mm diameter ESR quartz tubes using a JEOL JES-TE 300 spectrometer. The magnetic field was calibrated using the signal of Mn(II) ion

doped in MgO powder (g = 2.034 and 1.981). Experimental conditions: microwave frequency: 100 kHz, modulation amplitude: 10 G, and microwave power: 1.0 mW.

In a glove box, a solution of compound **1a** and **1b** (~ 10^{-3} M) was transferred to an EPR tube. The tube was capped with a rubber septum, removed from the glove box and stored in a cold bath (liq. N_2/ethanol) at -65 ^{o}C. Oxygenation reaction was carried out by directly bubbling the chilled solution with dry O_2 introduced via a syringe. The oxygenated solution was allowed to keep at this temperature for 10 min, after which the solution was frozen in liquid N_2 and excess O_2 was removed by evacuation and backfilling with N_2. The solution was then thawed in a cold bath (liq. N_2/ethanol) at -70 ^{o}C, and a solution of $CoCp_2$ and Fe^{II}-reduced form in THF was introduced via a syringe. The resultant solution was mixed completely by shaking the tube, and then it was frozen in liquid N_2 prior to spectral recording.

RR spectra were obtained on a SpectraPro-300i spectrometer (Acton Research) with a 2400-groove grating, a holographic Supernotch filter (Kaiser Optical Systems), and LN-1100PB CCD detector (Princeton Instruments) cooled with liquid N_2. Spectra were collected at an excitation wavelength λ_{ex} = 413.1 nm with spinning frozen sample positioned in a backscattering geometry. The procedure for rR sample preparation was the same as that of ESR sample described above by using of quartz NMR tubes. The sample was kept in liquid N_2 in a double-walled low-temperature quartz dewer. Power at the sample was less than 5 mW. Peak frequencies were calibrated relative to toluene and CCl_4 standards (accurate to ±1 cm^{-1}). For each rR sample, ESR spectra were also taken before and after the rR measurement, respectively.

Synthesis of the model compounds

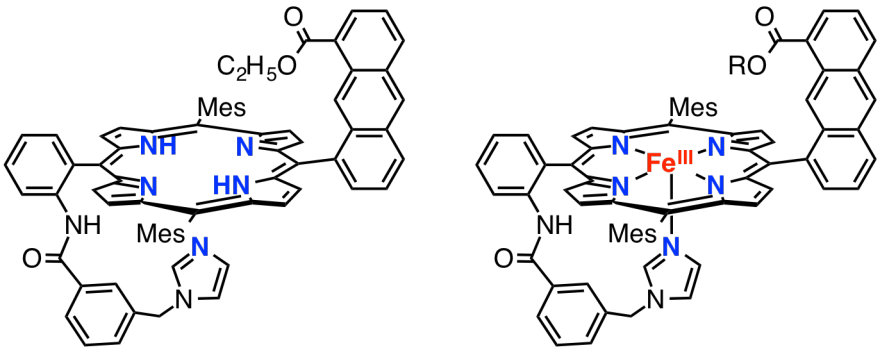

H_2L Fe^{III}-L1 (R = H)
Fe^{III}-L2 (R = Et)

Chart 1. Synthesized porphyrins.

5-({[3-Imidazole-1-yl]methyl}benzoylamido)phenyl)-15-[1-(2 ethoxycarbonylanthracene)]-10,20-dimesitylporphyrin (H_2L)

The synthesis of **H_2L** will be reported somewhere else.

^{1}H NMR ($CDCl_3$, 400 MHz): δ = 8.96 (s, 1H, Ar-H), 8.87 (d, 1H, Ar-H), 8.81 (d, 2H, *β*-H), 8.76 (s, 1H, Ar-H), 8.71 (d, 2H, *β* -H), 8.57 (dd, 4H, *β*-H), 8.45 (d, 1H, Ar-H), 8.25 (d, 1H, Ar-H), 8.2 (d, 1H, Ar-H), 8.18 (d, 1H, Ar-H), 8.14 (d, 1H, Ar-H), 7.9 (s, 1H, Ar-H), 7.89-7.85 (m, 2H, Ar-H), 7.71 (s, 1H, NH), 7.61 (t, 1H,Ar-H), 7.42 (s,1H, Ar-H), 7.22 (s, 4H, Ar-H), 6.99 (s, 1H, Im-H), 6.8 (s, 1H, Im-H), 6.51 (s, 1H, Im-H), 6.50 (d, 1H, Ar-H), 6.25 (t, 1H, Ar-H), 6.01 (d, 1H, Ar-H), 5.91 (t, 1H, Ar-H), 4.28 (s, 2H, CH_2), 2.8(q, 2H, OCH_2CH_3) , 2.6(s, 6H, CH_3), 1.81(s, 6H, CH_3), 1.79(s, 6H, CH_3), -1.04(t, 3H, OCH_2CH_3), -2.37(br, 2H, NH) ppm; **ESI-MS:** *m/z*: 1070.5 $[M+H]^+$; **HR-MS** (FAB, NBA): calcd. for $C_{72}H_{59}O_3N_7$: 1069.50; Found: 1070.48, $[M+H]^+$.

5-({[3-Imidazole-1-yl)methyl]benzoylamido}phenyl)-15-[1-(2-ethoxycarbonylanthracene)]-10,20-dimesitylporphyrinatoiron(III)bromide ([Fe^{III}L2]Br)

To a solution of H_2L (50 mg, 42 µmol) in deoxygenated THF (30 mL) at reflux was added $FeBr_2$ (36 mg, 168 µmol), and heating was continued for 3 h under N_2 atmosphere. After cooling the solution to r.t. the solution was opened to air and chloroform (40 mL) was added. The organic phase was treated with 2.0 N HCl, and washed with water (3 x 50 mL), and saturated NaBr solution, respectively. The organic phase was dried over anhydrous Na_2SO_4.

Removing the solvent under vacuum, and the resultant residue was purified by flash column chromatography (silica gel, MeOH/CH_2Cl_2, v/v = 5:95). Yield: 46 mg, 88 %. ESI-MS: m/z: 1124.4 $[M+H]^+$; HR-MS (FAB, NBA): calcd for $C_{72}H_{57}FeN_7O_3$: 1123.4; Found: 1123.39 $[M-Br]^+$. UV/Vis (THF): λ_{max} (ε) = 422 (8.8×10^4), 512 (9.0×10^3 M^{-1} cm^{-1}).

5-({[3-Imidazole-1-yl)methyl]benzoylamido}phenyl)-15-[1-(2-hydroxycarbonylanthracene)]-10,20-dimesitylporphyrinato-iron(III) bromide ([Fe^{III}L1]Br)

To a solution of ([Fe^{III}L2]Br) in THF (6 mL) added 2N LiOH aq. (416 µL, 0.832 mmol), and MeOH (3 mL) was refluxed under nitrogen atmosphere for 5 h. The solvent was removed by a rotary evaporator. The solids were redissolved in CH_2Cl_2 and washed with water. The organic layer was stirred with 3N HCl (1 mL), then washed with water. The organic phase was stirred with saturated NaBr solution for 20 min. The organic phase was dried over anhydrous Na_2SO_4. Removing the solvent under vacuum, and the resultant residue was purified by flash column chromatography (silica gel, MeOH/CH_2Cl_2, v/v = 2:98). Yield: 40 mg, 82%. ESI-MS: *m/z*: 1095.4 (100) [*M*-Br]$^+$; HR-MS (FAB, NBA): calcd for $C_{70}H_{53}FeN_7O_3$: 1095.4; Found: 1095.36 [*M*-Br]$^+$. UV/Vis (THF): λ_{max} (ε) = 418 (7.8×10^4 M^{-1} cm^{-1}).

Deuteration of [Fe^{III}L1]Br for preparation of Fe-OOD intermediate

In a glove-box, compound Fe^{III}-L1 (0.9 µmol) dissolved in 0.4 mL THF and 0.2 mL DCM mixture. To this solution added 1 mL D_2O, then stirred over night. Remove the solvent under vacuum, then add 2 mL DCM and separate aqueous layer. The organic layer was dried over anhydrous Na_2SO_4. Remove the solvent under vacuum and dry for 4h.

[Fe^{II}L1] (1a) and [Fe^{II}L2] (1b) Added 1 equiv. of cobaltocene in THF solution to the ([Fe^{III}L1]Br) and ([Fe^{III}L2]Br) in 80% EtCN/CH_2Cl_2 in a glove box.

[Fe^{II}L1] (1a) UV/vis : λ_{max} (ε) = 428 (9 x 10^4), 535 (1.9 x 10^4), 570 (7 x 10^3 $M^{-1}cm^{-1}$); ESI-MS: m/z: 1095.4

[Fe^{II}L2] (1b) UV/vis : λ_{max} (ε) = 428 (9.3 x 10^4), 535 (2 x 10^4), 570 (8.5 x 10^3 $M^{-1}cm^{-1}$); ESI-MS: m/z: 1123.4

Spectroscopic characterization of reaction intermediates

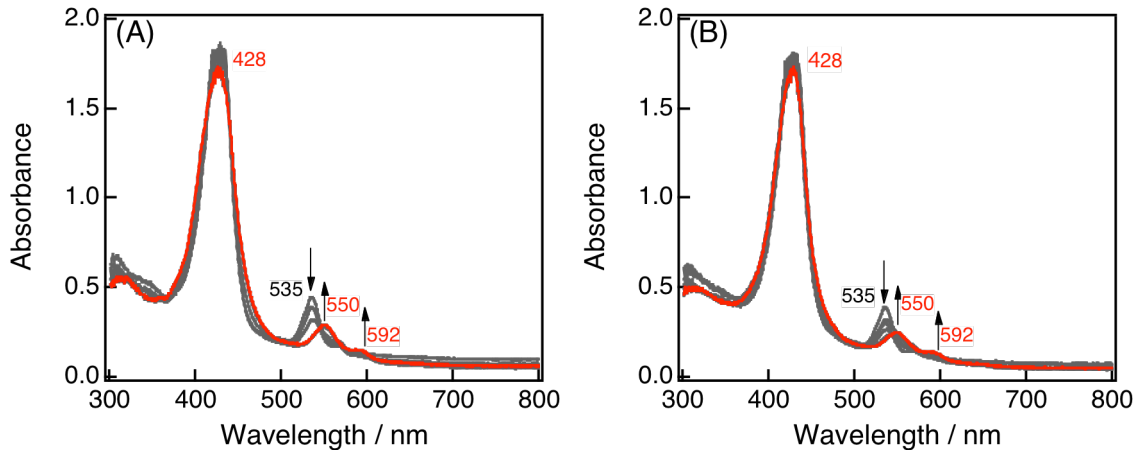

Figure S1. (A) UV-visible spectral changes of compound **1a** upon oxygenation to afford **2a** and (B) UV-visible spectral changes of compound **1b** upon oxygenation to afford **2b** in 80 % EtCN/CH_2Cl_2 at -65 ^oC. Spectral interval 1 min.

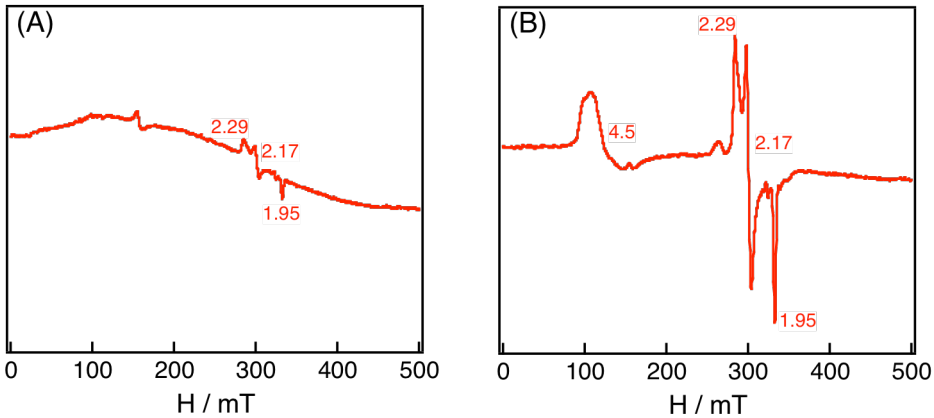

Figure S2. ESR spectra of (A) unexpected generation of compound **3a** upon oxygenation of compound **1a** in 80% EtCN/CH_2Cl_2 at -65 ^oC. (B) compound **4** and **3a** 1:1 generated by the addition of 1 equiv of compound **1a** to the solution of **2a** in 80% EtCN/CH_2Cl_2 at -70 ^oC.

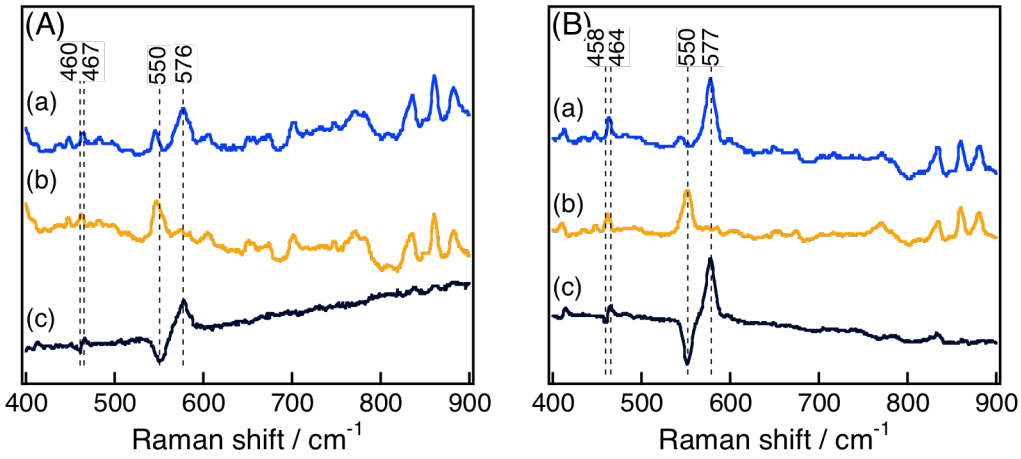

Figure S3. (A) rR spectra (λ_{ex}=413 nm, 77 K) of **2a** containing (a) ^{16}O and (b) ^{18}O and (c) their difference spectrum (a-b). (B) rR spectra (λ_{ex}=413 nm, 77 K) of **2b** containing (a) ^{16}O and (b) ^{18}O and (c) their difference spectrum (a-b).

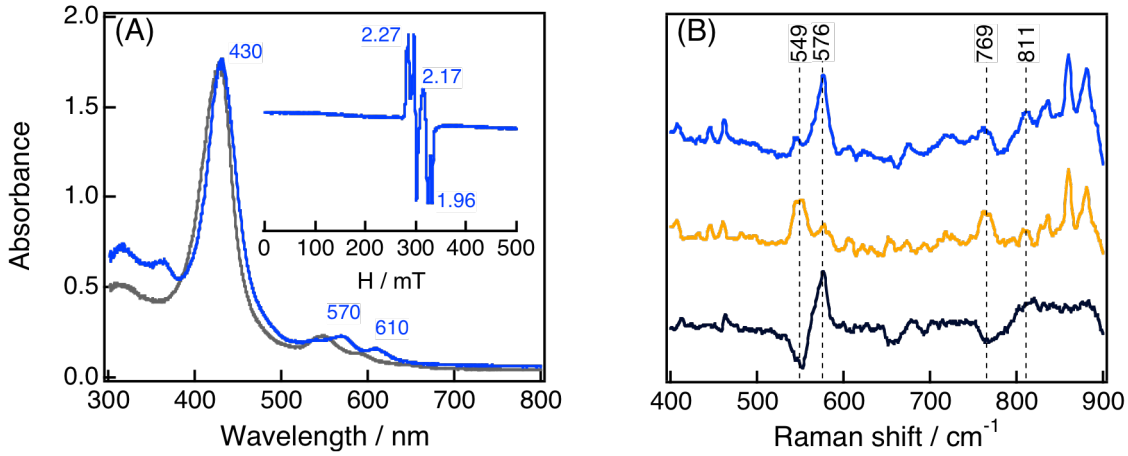

Figure S4. (A) UV-vis spectra of **3b** (red line) generated by addition of $CoCp_2$ and methanol to the solution of **2b** in 80% EtCN/CH_2Cl_2 at −70 °C. Inset: ESR spectrum of **3b** at 77 K. (B) rR spectra of **3b** generated by addition of $CoCp_2$/MeOH (300 equiv.) to the solution of **2b** in 80% EtCN/CH_2Cl_2 at -70 °C containing (a) ^{16}O and (b) ^{18}O and (c) difference spectrum of (a)-(b). λ_{ex} = 413 nm, 77 K.

Computational details

DFT computations were carried out using Jaguar version 7.7 program package.[1] Fully optimized molecular structures were obtained by geometry optimization at the BP86/LACV3P+* (Fe) and 6-311+G* (N and O (O_2)) and 6-31G* (other atoms) level, and calculation of Hessians at the same theory level were performed. Solvation energy calculations were carried out by using the Poisson-Boltzmann solver with propanonitrile (dielectric constant of 29.324 and probe radius of 2.41)[2] as a solvent on the optimized structures using the same theory level.

The geometry optimization of the acid complex was carried out using a model in which the carboxylic acid group donates a H-bond to heme-bound O_2 or O_2H ligands. The ester complex was modeled using a methoxy group, and conformational variants were taken into consideration as shown in Scheme 1: The methoxy group is pointed to the heme bound O_2 ligand in A mechanism, while the relative position of the methoxy and carbonyl is flipped in B mechanism. Comparison of the reaction mechanisms using these models should illuminate the role of the H-bond interaction in the O_2 activation.

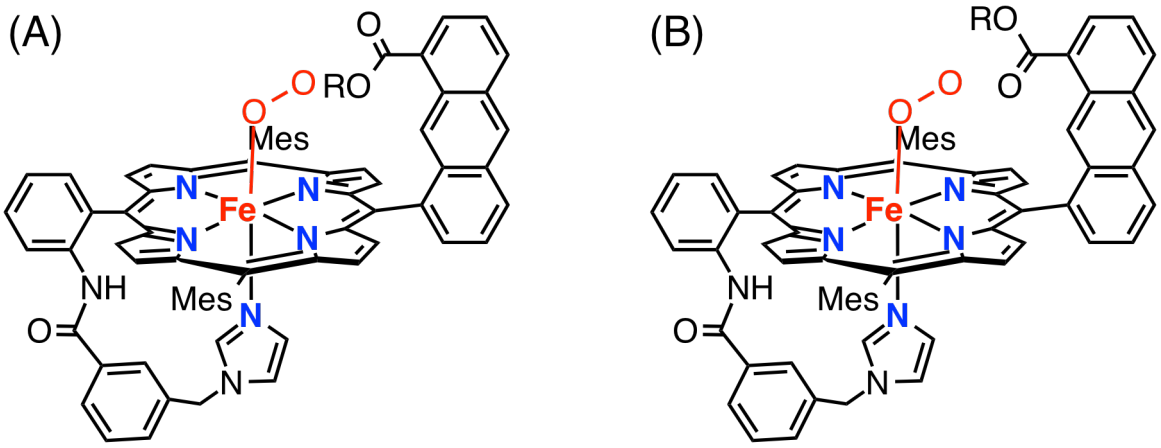

Scheme S1. Possible conformations of the ester complex A and B, where R represents CH_3.

A water molecule was included in the computational models of the acid and ester complexes, because a low concentration (a few ppm level) of water could remain in solvents even though it was dried carefully.[3] The complex **2** (ferric-superoxy species) and its protonated form was calculated in a broken symmetry method, in which α and β electron densities are allowed to localize on different atoms. The spin-projected correction developed by Yamaguchi[4] was carried out using equations 1 and 2 to take into consideration of relatively large spin contaminations of the broken-symmetry calculations.

$$E_s = (E_c - aE_{S+1}) / (1-a) \quad \text{(eq. 1)}$$

$$a = \left[\left\langle S^2 \right\rangle_c - s(s+1)\right] / 2(s+1) \quad \text{(eq. 2)}$$

E_c is the spin-contaminated energy for singlet state, E_{s+1} is the energy for the triplet state, $<S^2>_c$ is the calculated spin expectation value of the spin-contaminated singlet state.[5]

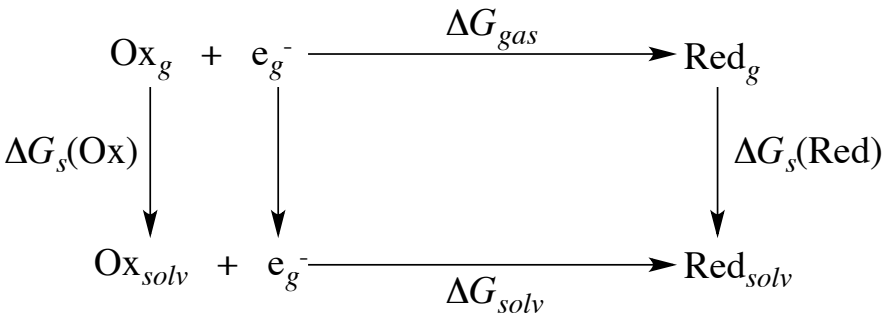

Scheme S2. Calculation of free energy changes of reduction under solvated conditions using a Born-Haber cycle.

The calculation of redox potential of molecules relies on free energy change between the reactant and one-electron oxidized or reduced species under solvated conditions. The frequently used procedure to calculate free energy change under solvation assumes Born-Haber cycle (Scheme S2), in which gas phase free energy change in redox reaction is first calculated and then the gas-phase energy is calibrated by the difference of solvation energy between the reactant and product as shown in equations 3 and 4.

$$\Delta G_{solv} = \Delta G_{gas} + \Delta G_s(Red) - \Delta G_s(Ox) \qquad \text{(eq. 3)}$$

$$\Delta G_{gas} = \Delta H_{gas} - T\Delta S_{gas} \qquad \text{(eq. 4)}$$

$$\Delta G_{solv} = -nFE^{\circ} \qquad \text{(eq. 5)}$$

In Scheme S2, Ox_g corresponds to the gas phase geometry optimized structure of ferric-superoxy heme, and Red_g is one-electron reduced species of Ox_g in the gas phase. The Nernst equation determines the standard one-electron redox potentials, E^o/V, as shown in equation 5, where F is the Faraday constant 23.06 kcal mol^{-1} V^{-1}. Calculations were carried out for gas-phase geometries employing dielectric constant of 29.324 (propanonitrile) for the solvating continuum medium. To correlate the computationally obtained redox potential with experimental data, referencing the calculated value with the standard hydrogen electrode potential in the organic solvent is necessary, for which 4.53 eV was used.[6,7]

Calculation of pKa is based on the equations 6-8. In equation 7, T corresponds to 228.5 K and k_B is the Boltzmann constant. The calculation of pK_a of molecules relies on free energy change between the reactant and protonated species under solvated conditions. The frequently used procedure to calculate free energy change under solvation assumes Born-Haber cycle (Scheme S3), in which gas phase free energy change in protonation is first calculated and then the gas-phase energy is calibrated by the difference of solvation energy between the reactant and product as shown in equation 8.

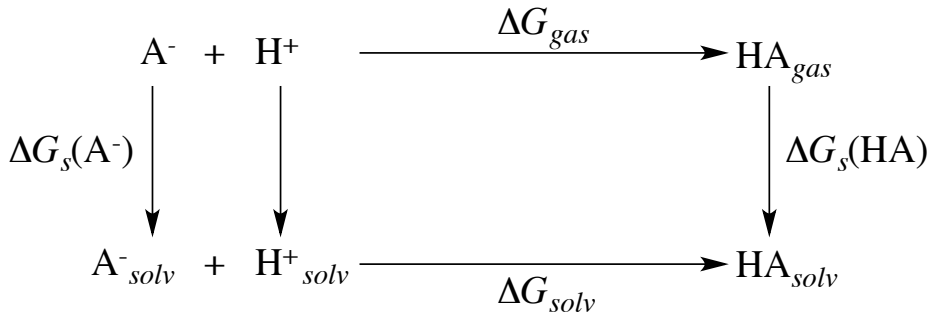

Scheme S3. Calculation of free energy changes of protonation under solvated conditions using a Born-Haber cycle.

$$\Delta G_{solv} = \beta p K_a \qquad \text{(eq. 6)}$$

$$\beta = k_B T \qquad \text{(eq. 7)}$$

$$\Delta G_{solv} = \Delta G_{gas} + \Delta G_s(A^-) + \Delta G_s(H^+) - \Delta G_s(HA) \qquad \text{(eq. 8)}$$

ΔG_{gas} (= ΔH_{gas}- $T\Delta S_{\text{gas}}$) is the free energy change due to the protonation in the gas phase. The solvation free energy of proton in the solvent was assumed as -257.2 kcal/mol to have consistency with the absolute potential of SHE in the organic solvent.[6,7]

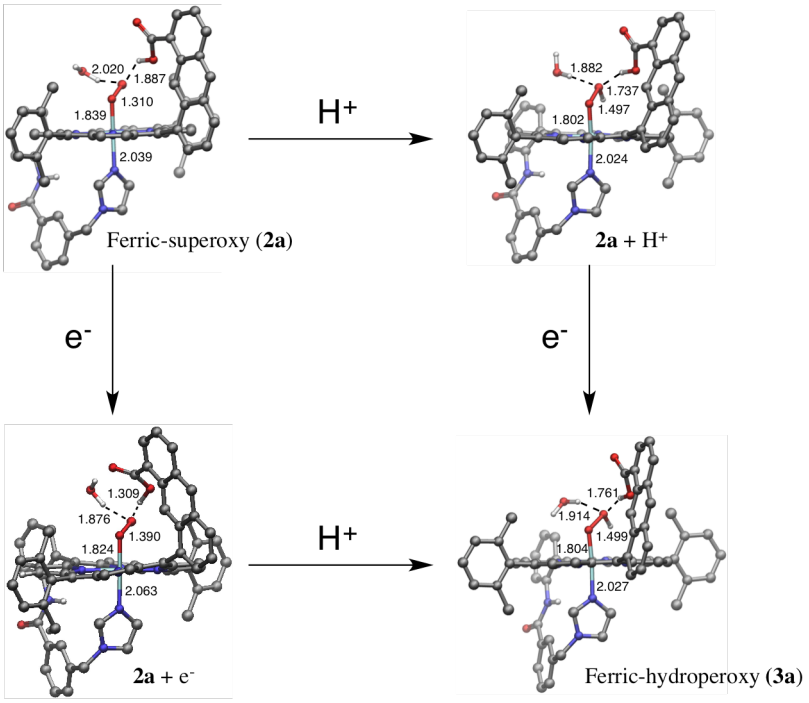

Figure S5. DFT optimized geometries of reaction intermediates involved in one-electron reduction and protonation of ferric-superoxy species of the acid complex.

Table S1. BP86 DFT calculated energies of the acid complex.[a]

	SCFE	G_{gas} [b]	ΔG_{sol}
2a	-3580.26894485959	-3579.329757	-27.6379
2a + 1e$^-$	-3580.36458933471	-3579.429474	-55.6211
2a+ H$^+$	-3580.67045140951	-3579.719124	-47.9663
4a	-3580.88881371644	-3579.937511	-28.333

[a] Units are in hartree except the solvation energy ΔG_{sol} in kcal/mol. [b] $G_{gas} = H_{tot}$-T•S, where in $H_{tot} = U_{tot} + pV$ and U_{tot} = SCFE + ZPE + U.

Table S2. DFT calculated energies for spin projected correction of **2a**.

State	**2a**	**2a + H$^+$**
Singlet (BS)	-3580.26894485959	-3580.67045140951
$<S^2>_{singlet}$	0.667	1.017
Singlet (Corrected)	-3580.271763	-3580.674854
Triplet	-3580.26331285092	-3580.66622159187
$<S^2>_{triplet}$	2.023	2.018

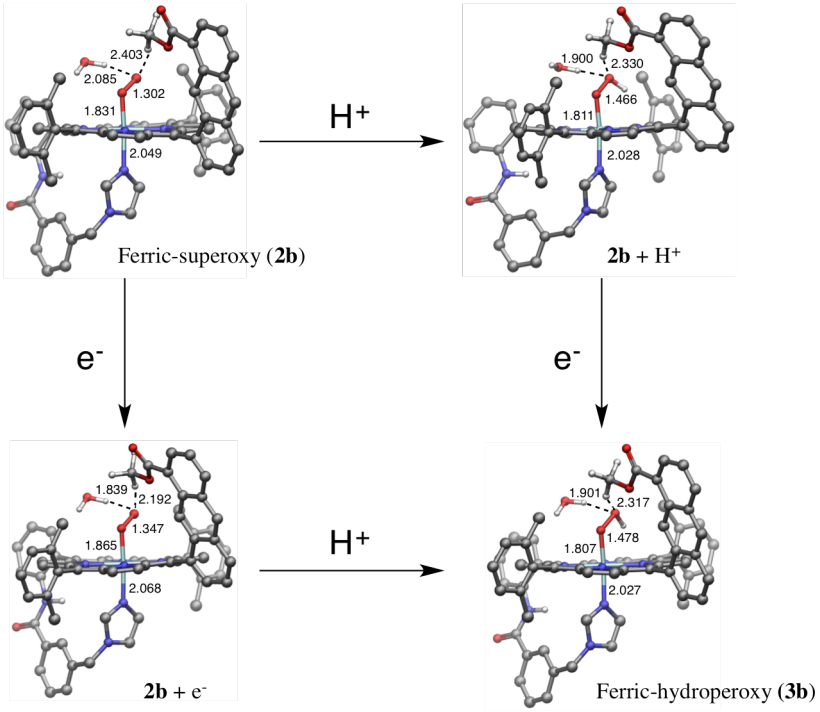

Figure S6. DFT optimized geometries of reaction intermediates involved in one-electron reduction and protonation of ferric-superoxy species of the ester complex (A-mechanism).

Table S3. BP86 DFT calculated energies of the ester complex in the A mechanism.[a]

	SCFE	G_{gas}[b]	ΔG_{sol}
2b	-3619.56610562442	-3618.600182	-26.5536
2b + 1e$^-$	-3619.65136120448	-3618.688087	-52.5356
2b + H$^+$	-3619.96601426557	-3618.991466	-48.4305
3b	-3620.18431483667	-3619.208122	-27.3818

[a] Units are in hartree except the solvation energy ΔG_{sol} in kcal/mol. [b] $G_{gas} = H_{tot}$-T•S, wherein $H_{tot} = U_{tot}$ + pV and U_{tot} = SCFE + ZPE + U.

Table S4. DFT calculated energies for spin projected correction of **2b** in the path A.

State	**2b**	**2b + H$^+$**
Singlet (BS)	-3619.56610562442	-3619.96601426557
$<S^2>_{singlet}$	0.641	0.962
Singlet (Corrected)	-3619.569398	-3619.966373
Triplet	-3619.55912619536	-3619.96562761973
$<S^2>_{triplet}$	2.025	2.021

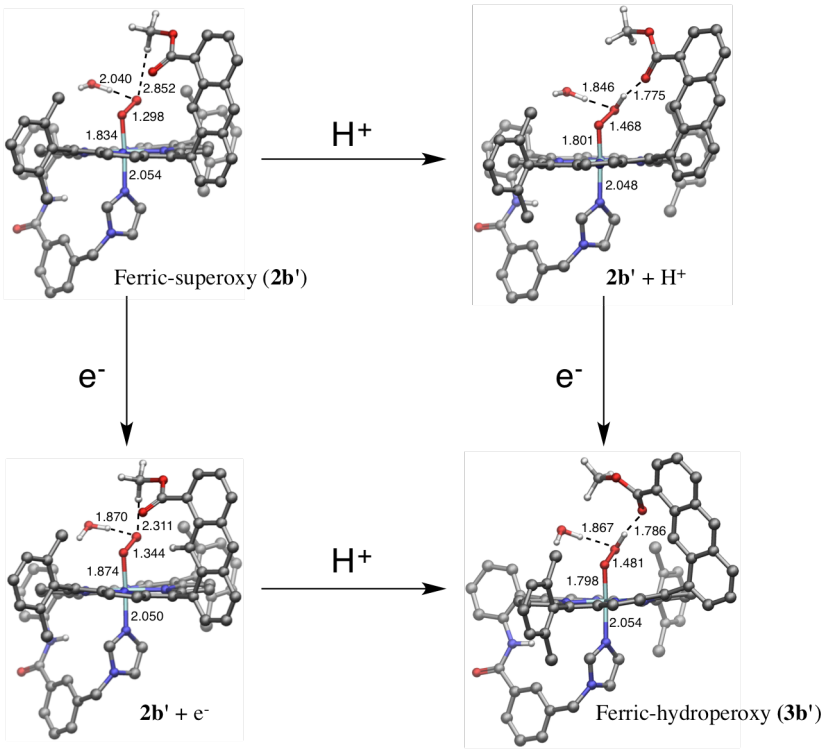

Figure S7. DFT optimized geometries of reaction intermediates involved in one-electron reduction and protonation of ferric-superoxy species of the ester complex (B mechanism).

Table S5. BP86 DFT calculated energies of ester model in the B mechanism.[a]

	SCFE	G_{gas}[b]	ΔG_{sol}
2b'	-3619.56547680567	-3618.602820	-25.0355
2b' + 1e$^-$	-3619.64676951113	-3618.684547	-51.9046
2b' + H$^+$	-3619.98089425841	-3619.005105	-44.9999
3b'	-3620.19281890382	-3619.214321	-24.8017

[a] Units are in hartree except the solvation energy ΔG_{sol} in kcal/mol. [b] $G_{gas} = H_{tot}$-T•S, wherein $H_{tot} = U_{tot}$ + pV and U_{tot} = SCFE + ZPE + U.

Table S6. DFT calculated energies for spin projected correction of **2b'** in the path B.

State	**2b'**	**2b' + H$^+$**
Singlet (BS)	-3619.56547680567	-3619.98089425841
$<S^2>_{singlet}$	0.664	1.021
Singlet (Corrected)	-3619.573697	-3619.980956
Triplet	-3619.54835023457	-3619.98085741373
$<S^2>_{triplet}$	2.032	2.022

Reference

[1] A. D. Bochevarov, E. Harder, T. F. Hughes, J. R. Greenwood, D. A. Braden, D. M. Philipp, D. Rinaldo, M. D. Halls, J. Zhang and R. A. Friesner, *Int. J. Quantum Chem.*, 2013, **113**, 2110.

[2] J. D. Thompson, C. J. Cramer and D. G. Truhlar, *J. Chem. Phys.*, 2003, **119**, 1661.

[3] D. B. G. Williams and M Lawton, *J. Org. Chem.*, 2010, **75**, 8351.

[4] K. Yamaguchi, F. Jensen, A. Dorigo, K. Houk, *Chem. Phys. Lett.* 1988, **149**, 537.

[5] H. Chen, M. Ikeda-Saito and S. Shaik, *J. Am. Chem. Soc.*, 2008, **130**, 14778-14790.

[6] S. Trasatti, *Pure. Appl. Chem.*, 1986, **58**, 955-966.

[7] A. A. Isse and A. Gennaro *J. Phys. Chem. B,* 2010**, 114**, 7894–7899.